



ELSEVIER

Available online at [www.sciencedirect.com](http://www.sciencedirect.com)

SCIENCE @ DIRECT®

Nuclear Instruments and Methods in Physics Research A 541 (2005) 398–404

NUCLEAR  
INSTRUMENTS  
& METHODS  
IN PHYSICS  
RESEARCH  
Section A

[www.elsevier.com/locate/nima](http://www.elsevier.com/locate/nima)

# Recent progress of avalanche photodiodes in high-resolution X-rays and $\gamma$ -rays detection

J. Kataoka<sup>a,\*</sup>, T. Saito<sup>a</sup>, Y. Kuramoto<sup>a</sup>, T. Ikagawa<sup>a</sup>, Y. Yatsu<sup>a</sup>, J. Kotoku<sup>a</sup>,  
M. Arimoto<sup>a</sup>, N. Kawai<sup>a</sup>, Y. Ishikawa<sup>b</sup>, N. Kawabata<sup>b</sup>

<sup>a</sup>*Tokyo Institute of Technology, 2-12-1 Ohokayama, Meguro, Tokyo 152-8551, Japan*

<sup>b</sup>*Hamamatsu Photonics K.K., Hamamatsu, Shizuoka, Japan*

Available online 19 February 2005

## Abstract

We have studied the performance of large area avalanche photodiodes (APDs) recently developed by Hamamatsu Photonics K.K. in high-resolution X-rays and  $\gamma$ -rays detections. We show that reach-through APD can be an excellent soft X-ray detector operating at room temperature or moderately cooled environment. We obtain the best energy resolution ever achieved with APDs, 6.4% for 5.9 keV X-rays, and obtain the energy threshold as low as 0.5 keV measured at  $-20^\circ\text{C}$ . Thanks to its fast timing response, signal carriers in the APD device are collected within a short time interval of 1.9 ns (FWHM). This type of APDs can therefore be used as a low-energy, high-counting particle monitor onboard the forthcoming Pico-satellite Cute1.7. As a scintillation photon detector, reverse-type APDs have a good advantage of reducing the dark noise significantly. The best FWHM energy resolutions of  $9.4 \pm 0.3\%$  and  $4.9 \pm 0.2\%$  were obtained for 59.5 and 662 keV  $\gamma$ -rays, respectively, as measured with a CsI(Tl) crystal. Combination of APDs with various other scintillators (BGO, GSO, and YAP) also showed better results than that obtained with a photomultiplier tube (PMT). These results suggest that APD could be a promising device for replacing traditional PMT usage in some applications. In particular 2-dim APD array, which we present in this paper, will be a promising device for a wide-band X-ray and  $\gamma$ -ray imaging detector in future space research and nuclear medicine.

© 2005 Elsevier B.V. All rights reserved.

PACS: 07.85; 95.55.A; 85.60.D

Keywords: Avalanche photodiode; Soft X-ray detector; Scintillation  $\gamma$ -ray detector; Imaging device

## 1. Introduction

In recent years avalanche photodiodes (APD) have attracted considerable attention since good features of both photodiodes (PDs) and photomultiplier tubes (PMTs) are shared by APDs [1].

\*Corresponding author. Tel.: +81 3 5734 2388;  
fax: +81 3 5734 2389.

E-mail address: [kataoka@hp.phys.titech.ac.jp](mailto:kataoka@hp.phys.titech.ac.jp) (J. Kataoka).

In fact, APDs have the quantum efficiency close to 100% in the visible and near infrared, can be very compact and less affected by magnetic field, and produces an internal gain of 10–100 or more, though it is much less than typical PMT gain. Thus the basic properties of APD is well suited to read out small numbers of photons, so long as it has large detection area and is operated under stable conditions.

For a long time, however, APDs were limited to very small surfaces, and mainly used as a digital device for light communications (e.g., a receiver for optical fibers). During the past decade, a large area APDs operating as a linear detector has also been available. As a scintillation photon detector, Moszyński et al. [2–4] have obtained a better or comparable energy resolution to those observed with a PMT. Moreover, operations of APDs at low temperature reduce the dark current noise contribution. This significantly improves the sensitivity to low-intensity signals, such as weak scintillation light produced by low energy X-rays.

In this paper, we report the performance of large area APDs recently developed by Hamamatsu Photonics K.K to determine its suitability as a low energy X-rays and  $\gamma$ -rays scintillation detector. After recalling APD structures, we summarize fundamental properties of three different APDs in Section 2. In Section 3, we present the performance of reach-through APD in direct detection of soft X-ray photons. In Section 4, we show the energy spectra of  $\gamma$ -ray sources measured with four different scintillators coupled to the reverse-type APDs. As a future imaging application, the performance of a pixel APD array will be presented in Section 5. Finally we summarize our results in Section 6.

## 2. APD structures and parameters

### 2.1. APD types

Three different types of APDs are now commercially available: (a) “beveled-edge”, (b) “reach-through”, and (c) “reverse-type” diode (Fig. 1). Structure (a), the “beveled-edge” diode is a traditional  $p^+n$  junction in which the  $n$ -type

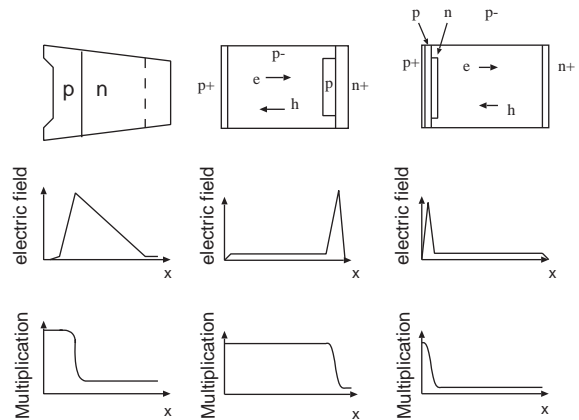


Fig. 1. Internal structures of three different types of APDs. (a) beveled-edge, (b) reach-through, and (c) reverse type (from left to the right). The electric field profiles and the gain profiles in each APDs are also shown in the middle and bottom panels.

resistivity is chosen so as to make the breakdown voltage very high (typically 2000 V) [2–7].

Structure (b), “reach through” type, applies to a diode in which the depletion layer comprises both a relatively wide drift region of fairly low field ( $\sim 2 \text{ V}/\mu\text{m}$ ) and a relatively narrow region of field sufficient for impact ionization ( $25\text{--}30 \text{ V}/\mu\text{m}$ ). The advantage of such a structure is that only relatively low voltages are required to full depleting the devices. Traditional reach-through APDs have a wide low-field drift region ( $\sim 100 \mu\text{m}$ ) at the front of the device, with the multiplying region at the back. A disadvantage is that most of the dark current undergoes electron multiplication, resulting that large area devices tend to be somewhat noisy.

The “reverse type (c)” is specifically designed to couple with scintillators. This type is quite similar to the reach-through APD, but the narrow high-field multiplying region has been moved to the front end, typically about  $5 \mu\text{m}$  from the surface of the device [8,9]. Since major scintillators emit at wavelength of 500 nm or less, most of lights from scintillators are absorbed within the first 1–3  $\mu\text{m}$  of the depletion layer and generates electrons which undergo full multiplication. Whereas most of the dark current undergoes only hole multiplication, reducing the noise contribution significantly.

Table 1  
Parameters for Hamamatsu APDs

Name	SPL 2407	S8664-55	S8664-1010
Type	(b)	(c)	(c)
Surface area	$\phi$ 3 mm	$5 \times 5 \text{ mm}^2$	$10 \times 10 \text{ mm}^2$
Dark current: $I_D$	4.4 nA	0.4 nA	1.7 nA
Capacitance: $C_{\text{det}}$	10.2 pF	88 pF	269 pF
Breakdown: $V_{\text{brk}}$	647 V	390 V	433 V

In this paper, we summarize the basic properties of APDs most recently developed by Hamamatsu (see Table 1): SPL2407, S8664-55, and S8664-1010. SPL2407 is a reach-through type, whereas S8664-55 and S8664-1010 are the reverse-type APDs. SPL 2407 ( $\phi$  3 mm) has a depletion layer of 130  $\mu\text{m}$  thickness, and can be used in direct detection of soft X-rays below 20 keV.

## 2.2. Gain and dark current

The gain characteristic of APDs can be measured under constant illumination of monochromatic light source recording the photocurrent of the APD as a function of bias voltage. We use a light emitting diode (LED) producing light signals of 525 nm. At voltages lower than 50 V (10 V for SPL 2407), the APD gain can be regarded as unity since the photocurrent remained constant. Fig. 2 shows variations of APD gain as a function of bias voltage, measured at  $+20^\circ\text{C}$ . At a gain of 30, the gain variations on bias voltage are approximated by  $+2.7\%/V$  for reverse-type APDs (S8664-55, S8664-1010) whereas  $+0.5\%/V$  for reach-through APD (SPL2407). Note that this is comparable to the voltage coefficient of typical PMTs ( $\sim +2\%/V$ ).

As discussed in detail in Ikagawa et al. [10] APD gain also depends on temperature. At a gain of 50, gain variations of APD ranges in a few  $\%/^\circ\text{C}$ , which is an order of magnitude larger than typical PMTs. Therefore, temperature control could be more critical problems for APDs. Throughout this paper, temperature was controlled in a thermostat within  $0.1^\circ\text{C}$ . The corresponding deviation in gain is less than 0.3%.

The leakage currents were measured at room temperature: 4.4, 0.4, and 1.7 nA at a gain of 30 for

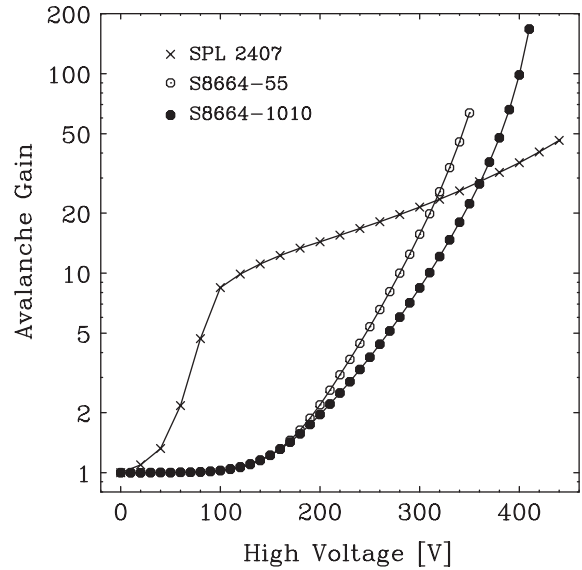


Fig. 2. Gain variations of Hamamatsu APDs measured at room temperature ( $+20^\circ\text{C}$ ).

SPL 2407, S8664-55 and S8664-1010, respectively. These values are extremely low compared to those reported for the beveled-edge APDs of a similar size. For example Moszyński et al. [2] reported that leakage current of  $\phi$  16 mm APD is  $\geq 100$  nA at room temperature. Regarding the Hamamatsu APDs, leakage current further decreases to 10–100 pA level at  $-20^\circ\text{C}$ .

## 3. Performance as a soft X-ray detector

### 3.1. Energy spectra

A reach-through APD of a 130  $\mu\text{m}$  thickness can potentially detect soft X-rays below 20 keV with efficiencies greater than 10%. The signal amplification in the APD devices has a good advantage of detecting soft X-rays even at room temperature or at lightly cooled environment [11,12]. Fig. 3 presents the energy spectrum of 5.9 keV X-rays from a  $^{55}\text{Fe}$  source measured with SPL 2407 at  $-20^\circ\text{C}$ . Note that energy threshold is as low as  $E_{\text{th}} \sim 0.5$  keV. The K-shell peaks of Mn  $K_\alpha$  and  $K_\beta$  are marginally resolved in the line profile. The FWHM width of the 5.9 keV peak was

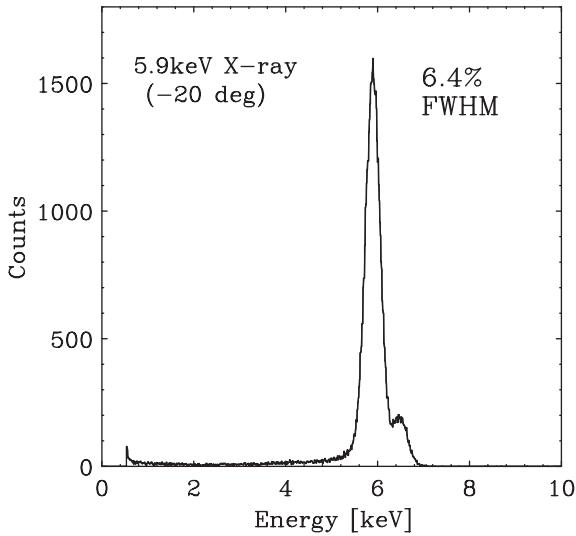


Fig. 3. Energy spectrum of 5.9 keV X-rays at  $-20^{\circ}\text{C}$ .

$\Delta E \sim 379\text{ eV}$  (6.4%; Fig. 3), which is the best record ever achieved with APDs. This resolution is clearly better than those obtained with the proportional counters.

### 3.2. High-rate counting

Fast timing is another excellent property of APDs. It has been reported that an APD with a few [square millimeter] detection area has fast timing properties better or comparable to that of a fast PMT [13,14]. We found that signal carriers in the APD device, SPL 2407, are collected within a short time interval of 1.9 ns (FWHM). Fig. 4 presents the output count rate as a function of the input (observed) photon rate for 8.0 keV photons. When setting a threshold as low as 1 keV for these 1.9 ns (FWHM) pulses, more than 34% signals were successfully recorded at the maximum input rate of  $\sim 3 \times 10^8$  cts/s. Note that the reduction of observed count rate is exactly consistent with that expected from the Poisson distribution with a dead time  $\tau \simeq 3.6$  ns (about twice of 1.9 ns), and is not due to the saturation of readout electronics. Since the noise level of the APD detector is less than  $10^{-2}$  cts/s, we obtain a dynamic range of more than  $10^9$ .

Since this type of APD (reach-through type) can also work as a charged particle detector, we plan

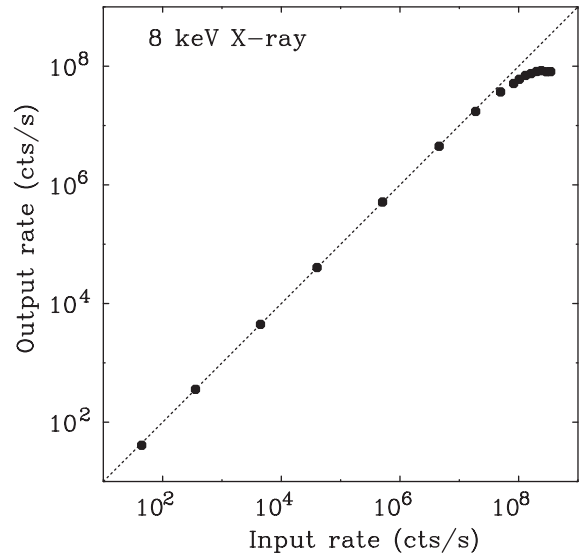


Fig. 4. Output count rate as a function of the input (observed) photon rate for 8.0 keV X-rays.

to use it as a high-counting particle monitor onboard the forthcoming Pico-satellite Cute1.7 [15]. This will be the first mission of using APDs in space as a scientific instrument, and study the distribution of low-energy ( $E \leq 30$  keV) electrons and protons trapped in the South Atlantic Anomaly (SAA) and aurora band.

## 4. Performance as a scintillation photon detector

### 4.1. Read-out of various scintillators

We study the performance of reverse-type APD, S8664-1010, as a  $\gamma$ -ray detector coupled with four different scintillators; CsI(Tl), BGO, GSO(Ce) and YAP(Ce). A size of the crystals was  $10 \times 10 \times 10\text{ mm}^3$ , and can fully match the sensitive area of the APD. Fig. 5 compares the pulse height spectra for 662 keV  $\gamma$ -rays from a  $^{137}\text{Cs}$  source, measured with a CsI(Tl) crystal at room temperature ( $+20^{\circ}\text{C}$ ). Thanks to its high quantum efficiency of more than 80%, an excellent FWHM energy resolution of  $4.9 \pm 0.2\%$  was obtained for the APD (*upper*). This is much better than that obtained with the 1-in PMT (*lower*:  $5.9 \pm 0.1\%$  FWHM; Hamamatsu R7899EG), where the

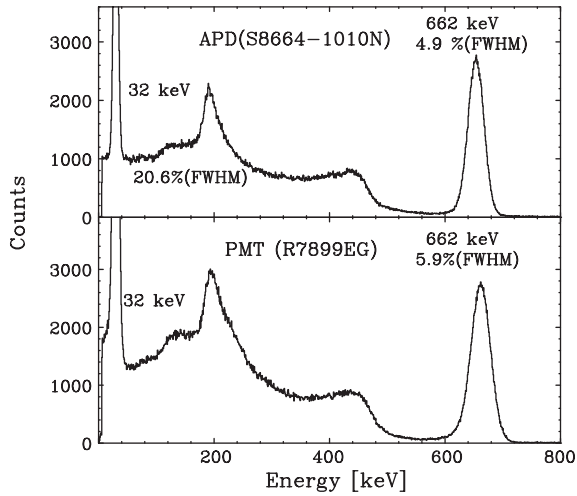


Fig. 5. Energy spectrum of  $^{137}\text{Cs}$  obtained with CsI(Tl) crystal coupled to a large area APD (S8664-1010: *top*) and PMT (R7899EG: *bottom*), measured at  $+20^\circ\text{C}$ .

quantum efficiency of R7899EG is more than 25% between 350 and 450 nm and the signal gain is  $\sim 1 \times 10^6$  at an operating bias voltage of 1000 V. More strikingly, APDs' internal gain reduces electric noise contribution significantly, resolving K-shell X-ray peak at 32 keV with the energy resolution of  $20.6 \pm 0.2\%$  ( $23.0 \pm 0.1\%$  for the PMT) [16].

Similarly, the large area APD is superior to the PMT when coupled with various scintillators (BGO, GSO(Ce), YAP(Ce)) as listed in Table 2. A good energy resolution of  $7.1 \pm 0.2\%$  was obtained for 662 keV  $\gamma$ -rays, as measured with BGO crystal at  $-20^\circ\text{C}$ . The minimum detectable energy was 11.3 keV.

#### 4.2. Low energy scintillation detection

Low leakage current of the reverse-type APD should have an excellent advantage for the detection of a low level of scintillation light, corresponding to  $\gamma$ -ray energy below 100 keV. To demonstrate the advantage of reverse-type APDs, we measured a CsI(Tl) crystal ( $5 \times 5 \times 5 \text{ mm}^3$ ) which can fully match the sensitive area of the S8664-55.

Fig. 6 shows the pulse height spectrum of 59.5 keV  $\gamma$ -rays from an  $^{241}\text{Am}$  source, measured

Table 2  
FWHM energy resolutions for 662 keV  $\gamma$ -rays

Crystal	APD ( $+20^\circ\text{C}$ ) (%)	APD ( $-20^\circ\text{C}$ ) (%)	PMT ( $+20^\circ\text{C}$ ) (%)
CsI(Tl)	$4.9 \pm 0.2$	$5.9 \pm 0.1$	$5.9 \pm 0.1$
BGO	$8.3 \pm 0.2$	$7.1 \pm 0.2$	$10.4 \pm 0.1$
GSO(Ce)	$7.8 \pm 0.2$	$7.1 \pm 0.2$	$9.3 \pm 0.1$
YAP(Ce)	$11.3 \pm 0.3$	$10.7 \pm 0.2$	$12.4 \pm 0.1$

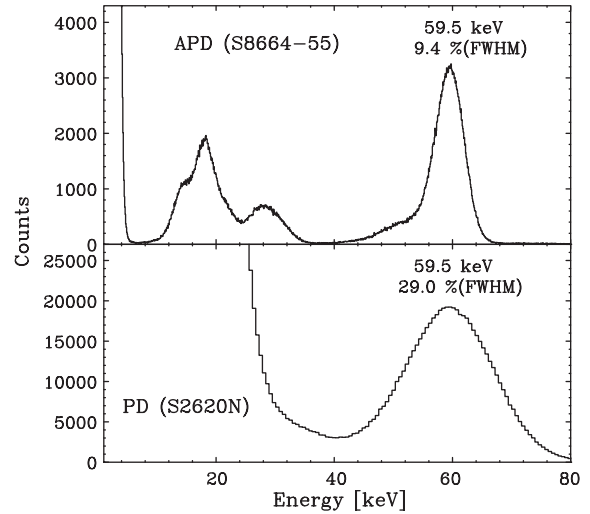


Fig. 6. Energy spectra of 59.5 keV  $\gamma$ -rays from a  $^{241}\text{Am}$  source measured with a CsI(Tl) crystal coupled to the APD (S8664-55: *upper*) and the PD (S2620N).

at room temperature [10]. The pulse height spectra, using the same CsI(Tl) scintillator coupled to the PIN-photodiode (Hamamatsu S2620N-1771:  $5 \times 5 \text{ mm}^2$  surface) is also shown for comparison. A combination of 14–21 keV lines of Np ( $L_\alpha$ ,  $L_\beta$  and  $L_\gamma$ ) is clearly resolved for APD whereas noise dominates for PIN-PD. Energy resolutions of 59.5 keV  $\gamma$ -rays are  $9.4 \pm 0.3\%$  for the APD and  $29.0 \pm 0.2\%$  for the PIN-PD, respectively. These results are one of the best records ever achieved with scintillation detectors. The minimum detectable energy is as low as 4.6 keV at room temperature, and improves significantly to 1.1 keV when cooled at  $-20^\circ\text{C}$ .

## 5. Applications: 32ch APD array

Finally, we tested a pixel APD array which offer new design options for physics experiments and nuclear medicine, such as imaging devices for positron emission tomography (PET). Hamamatsu S8550 (reverse-type) is a monolithic  $8 \times 4$  pixels structure with a surface area of  $2 \times 2 \text{ mm}^2$  for each pixel. The common cathode and the individual anode of the 32 diodes are connected at the backside of the carrier plates. We are testing the

performance of S8550, and are developing readout electronics for imaging purposes. Initial results are also found in literature [12,17].

The leakage current of S8550 is quite uniform between 16 pixels: 1.4–1.9 nA at a gain of 50, measured at  $\lambda = 420 \text{ nm}$ . Capacitance of each pixel ranges in 9–11 pF. Fig. 7 presents energy spectra obtained for 32 pixels of S8550 using 5.9 keV X-rays. The pixel-to-pixel gain non-uniformity was measured to be less than  $\pm 3\%$  at a gain of 50. Also one can clearly see that the energy threshold is as low as 0.8 keV for each pixels even at a room temperature. Kapusta et al. [17] reported that highest crosstalk between adjacent pixels was 4% at a device gain of 60. These reports promise the applicability of Hamamatsu APD array in nuclear medicine and space experiments near future. We are developing a  $\gamma$ -ray imaging detector based on the pixel APD arrays coupled to CsI(Tl) crystals, and results will be summarized in Saito et al. [18].

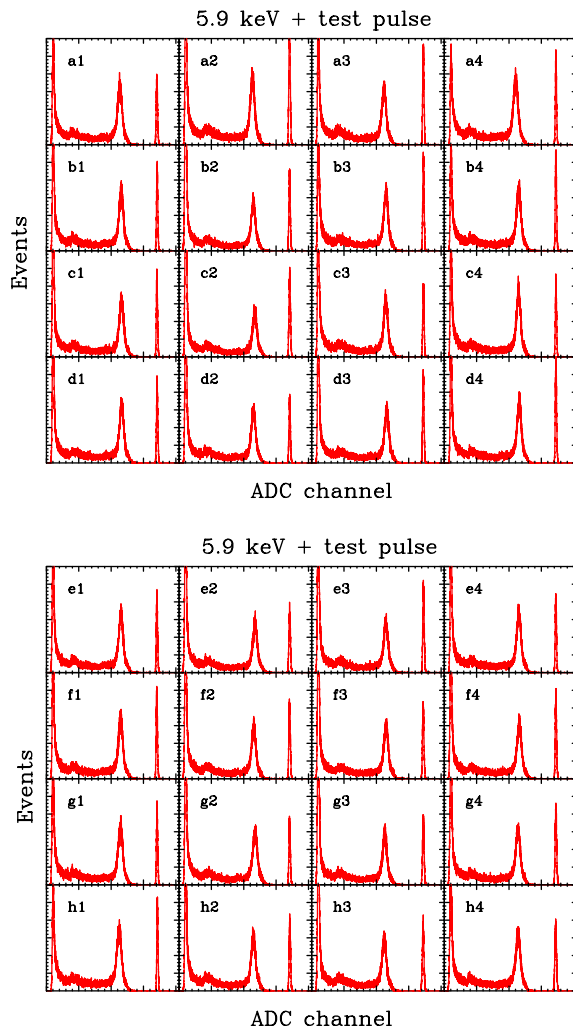


Fig. 7. A matrix of  $^{55}\text{Fe}$  (5.9 keV) spectra taken with each individual pixels of APD array.

## 6. Conclusion

We have studied the performance of large area APDs recently developed by Hamamatsu Photonics K.K. We showed that reach-through APD can be an excellent soft X-ray detector operating at room temperature or moderately cooled environment. We obtain the best energy resolution ever achieved with APDs, 6.4% for 5.9 keV X-rays, and obtain the energy threshold as low as 0.5 keV measured at  $-20^\circ\text{C}$ . As a scintillation photon detector, reverse-type APDs have a great advantage of reducing the dark noise significantly. We obtain the best FWHM energy resolutions of  $4.9 \pm 0.2\%$  and  $9.4 \pm 0.3\%$  for 662 and 59.5 keV  $\gamma$ -rays, respectively, as measured with a CsI(Tl) crystal. Combination of APDs with various other scintillators (BGO, GSO, and YAP) also showed better results than those obtained with the PMT. These results suggest that APD can be a promising device for replacing traditional PMT usage in some applications. In particular, pixel APD arrays offer new design options for future imaging devices.

**References**

- [1] P.P. Webb, R.J. McIntyre, J. Cornadi, *RCA Rev.* 35 (1974) 234.
- [2] M. Moszyński, M. Kapusta, D. Wolski, M. Szawłowski, W. Klamra, *IEEE Trans. Nucl. Sci.* NS-45 (1998) 472.
- [3] M. Moszyński, M. Kapusta, M. Balcerzyk, M. Szawłowski, D. Wolski, I. Wegrecka, M. Wegrzecki, *IEEE Trans. Nucl. Sci.* NS-48 (2001) 1205.
- [4] M. Moszyński, M. Szawłowski, M. Kapusta, M. Balcerzyk, *Nucl. Instr. and Meth. A* 497 (2003) 226.
- [5] A. Ochi, Y. Nishi, T. Tanimori, *Nucl. Instr. and Meth. A* 378 (1996) 267.
- [6] M. Moszyński, M. Kapusta, J. Zalipska, M. Balcerzyk, D. Wolski, M. Szawłowski, W. Klamra, *IEEE Trans. Nucl. Sci.* NS-46 (1999) 880.
- [7] M. Moszyński, W. Czarnacki, M. Szawłowski, B.L. Zhou, M. Kapusta, D. Wolski, P. Schotanus, *IEEE Trans. Nucl. Sci.* NS-49 (2002) 971.
- [8] R. Lecomte, C. Pepin, D. Rouleau, H. Dautet, R.J. McIntyre, D. McSween, P. Webb, *Nucl. Instr. and Meth. A* 423 (1999) 92.
- [9] R.J. McIntyre, P.P. Webb, H. Dautet, *IEEE Trans. Nucl. Sci.* NS-43 (1996) 1341.
- [10] T. Ikagawa, J. Kataoka, Y. Yatsu, et al., in preparation.
- [11] Y. Yatsu, J. Kataoka, Y. Kuramoto, et al., *Nucl. Instr. and Meth.* (2004), submitted for publication.
- [12] J. Kataoka, et al., *SPIE* 5501 (2004) 249.
- [13] S. Kishimoto, N. Ichizawa, T.P. Vaalsta, *Rev. Sci. Instr.* 69 (2) (1998) 384.
- [14] S. Kishimoto, H. Adachi, M. Ito, *Nucl. Instr. and Meth. A* 467–468 (2001) 1171.
- [15] Y. Kuramoto, et al., in preparation.
- [16] T. Ikagawa, J. Kataoka, Y. Yatsu, et al., *Nucl. Instr. and Meth. A* 538 (1–3) (2005) 640.
- [17] M. Kapusta, P. Crespo, D. Wolski, M. Moszyński, W. Enghardt, *Nucl. Instr. and Meth. A* 504 (2003) 139.
- [18] T. Saito, et al., in preparation.